

## Supporting Information

### High-sensitive Solid Chemical Sensor for Veterinary Drugs Based on Synergism Between Hydrogen Bond and Low-Dimensional Polymer Networks

Junhua Kuang,<sup>a,b</sup> Jie Yang,<sup>c</sup> Kai Liu,<sup>a,b</sup> Zhiyuan Zhao,<sup>a</sup> Wei Shi,<sup>a</sup> Mingchao Shao,<sup>a,b</sup> Yangshuang Bian,<sup>a,b</sup> Yanwei Liu,<sup>a,b</sup> Jinyang Chen,<sup>a,b</sup> Mingcong Qin,<sup>a,b</sup> Lang Jiang,<sup>a</sup> Jichen Dong,<sup>a</sup> Yunlong Guo\*<sup>a</sup> Yunqi Liu<sup>a</sup>

<sup>a</sup> Beijing National Laboratory for Molecular Sciences, CAS Key Laboratory of Organic Solids, Institute of Chemistry, Chinese Academy of Sciences, Beijing 100190, China

<sup>b</sup> University of Chinese Academy of Sciences, Beijing 100049, China

E-mail: guoyunlong@iccas.ac.cn

<sup>c</sup> Department of Materials Science and Engineering, City University of Hong Kong, Kowloon, Hong Kong SAR 999077, China

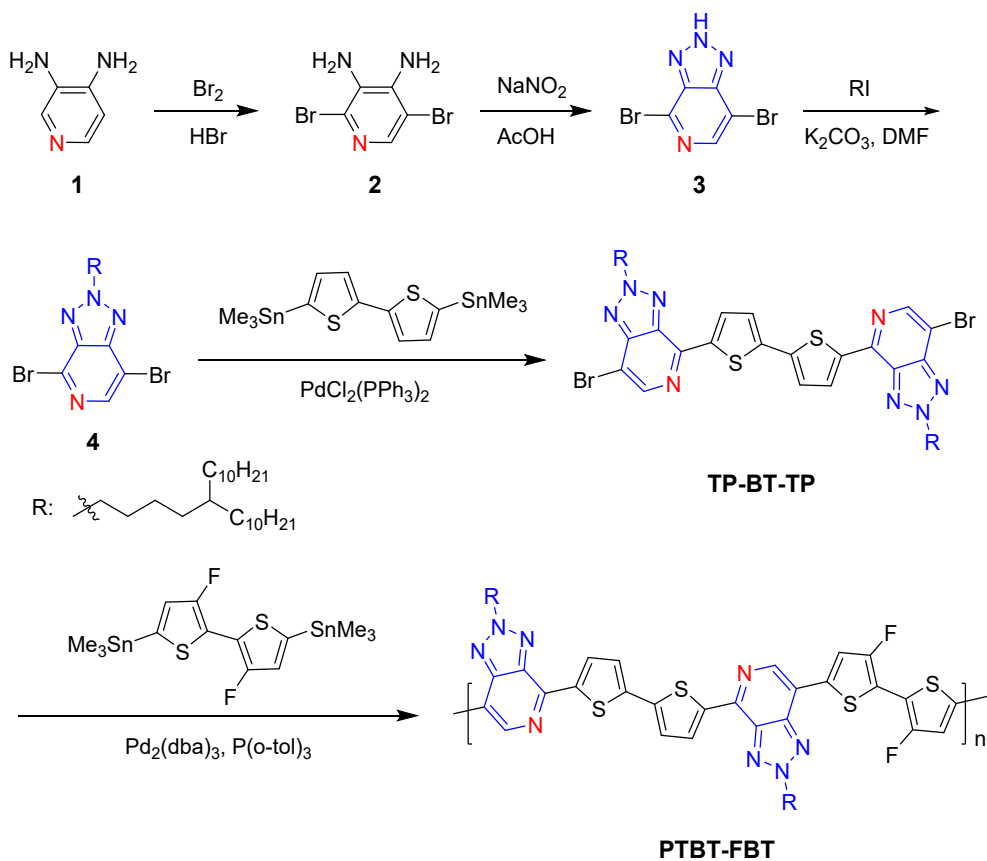
### Table of Contents

- 1. Materials Synthesis**
- 2. Experimental details**
- 3. Theoretical calculation**
- 4. Device fabrication and testing**
- 5. Figures S1-S19 and Table S1-S6**
- 6. Reference**

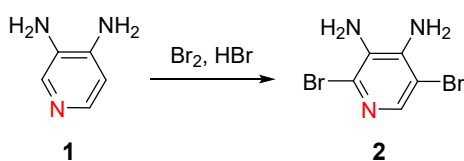
## 1. Materials Synthesis

### Synthesis of PTBT-FBT

**Reagents:** All starting reagents were purchased from Aldrich, Acros, or Alfa Aesar and used directly without further purification. **Compound 4**<sup>[1]</sup> was synthesized according to the literature.

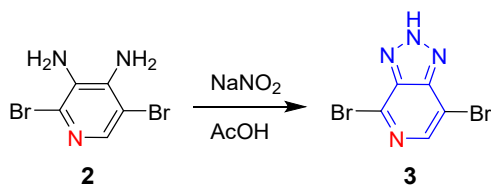


**Scheme S1.** The route to PTBT-FBT.

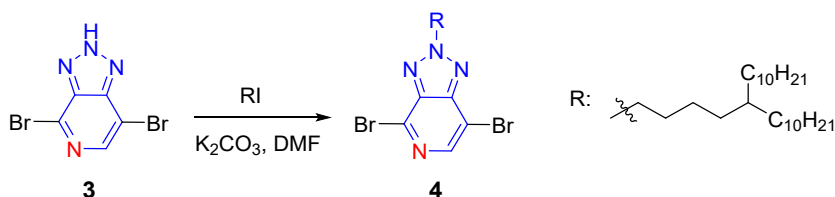


**Compound 2:** 3,4-diaminopyridine (**1**) (8.0 g, 73.3 mmol) was dispersed in aqueous hydrobromic acid (160 mL, 48%), and 9.8 mL bromine (30.6 g, 191.5 mmol) was added dropwise to the mixture at room temperature. The mixture was stirred at 110 °C for 4 h, and then cooled to 0 °C. A precipitate formed and was separated by filtration. The precipitate was washed with an aqueous solution of  $\text{Na}_2\text{S}_2\text{O}_3$ , an aqueous solution of  $\text{NaHCO}_3$ , and distilled water in the order. Then the slurry was extracted with  $\text{EtOAc}$  and  $\text{H}_2\text{O}$ . The organic phase was dried with  $\text{Na}_2\text{SO}_4$  and the solvent was removed, yielding **2** as a crystalline solid (8.0 g, 41 %).

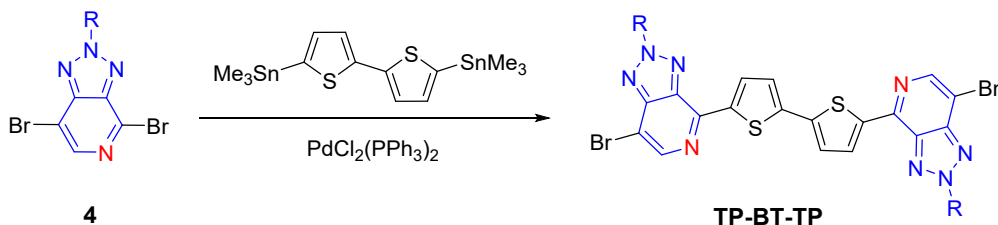
$^1\text{H NMR}$  (300 MHz,  $(\text{CD}_3)_2\text{SO}$ )  $\delta$  7.53 (s, 1H), 6.00 (s, 2H), 5.05 (s, 2H).  $^{13}\text{C NMR}$  (75 MHz,  $(\text{CD}_3)_2\text{SO}$ )  $\delta$  139.7, 138.9, 129.3, 126.4, 105.0. HREI:  $[\text{M}]^+$  calcd for  $\text{C}_5\text{H}_5\text{Br}_2\text{N}_3$ : 266.8830, found: 266.8833.



**Compound 3:** To an AcOH (250 mL) solution of **2** (15.0 g, 56.2 mmol), a solution of NaNO<sub>2</sub> (5.82 g, 84.3 mmol) in 90 mL of H<sub>2</sub>O was added. The mixture was stirred at 25 °C for 12 h. The suspension was filtered and rinsed with water and ethanol, giving the title product **3** (11.0 g, 71%) as a solid. The crude product was used for next reaction without further purification.

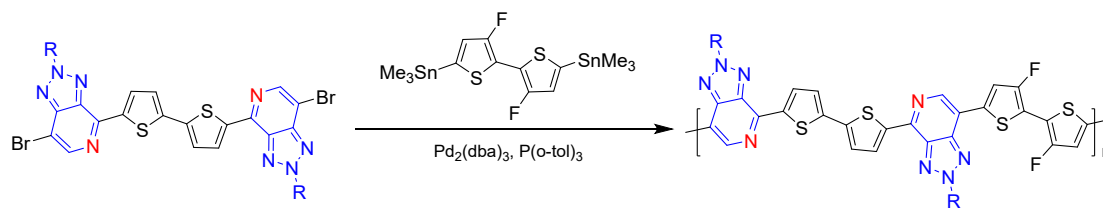


**Compound 4:** To a anhydrous *N,N'*-dimethylformamide (DMF) (250 mL) solution of **3** (8.00 g, 28.8 mmol) and K<sub>2</sub>CO<sub>3</sub> (7.96 g, 57.6 mmol), 1-iodo-5-decylpentadecane (16.54 g, 34.6 mmol) was added. The mixture was stirred at 90 °C for 24 h under nitrogen. The solution was extracted with CH<sub>2</sub>Cl<sub>2</sub> and then washed with water and brine, and dried over with Na<sub>2</sub>SO<sub>4</sub>. After removal of the solvent under reduced pressure, the crude product was purified by silica gel chromatography with eluent (PE: CH<sub>2</sub>Cl<sub>2</sub> = 5: 1) to give **4** as an oil (9.45 g, 52%). <sup>1</sup>H NMR (300 MHz, CDCl<sub>3</sub>) δ 8.34 (s, 1H), 4.83 (t, *J* = 7.5 Hz, 2H), 2.15 (m, 2H), 1.60–1.00 (m, 41H), 0.88 (m, 6H). <sup>13</sup>C NMR (75 MHz, CDCl<sub>3</sub>) δ 146.4, 143.3, 141.7, 132.7, 108.1, 58.1, 37.2, 33.5, 32.9, 31.9, 30.5, 30.1, 29.7, 29.6, 29.4, 26.6, 23.6, 22.7, 14.1. HR-MALDI-TOF: [M+H]<sup>+</sup> calcd for C<sub>30</sub>H<sub>53</sub>Br<sub>2</sub>N<sub>4</sub>: 629.26166, found: 629.26116.



**TP-BT-TP:** A Schlenk flask was charged with **4** (1.20 g, 1.9 mmol), 5,5'-bis(trimethylstannyl)-2,2'-bithiophene (0.47 g, 0.95 mmol) and catalytic amount of PdCl<sub>2</sub>(PPh<sub>3</sub>)<sub>2</sub> (33.6 mg) under nitrogen. 40 mL of degassed chlorobenzene was added. The mixture was stirred for 24 h at 110 °C under nitrogen. Then the solution was cooled to room temperature, the solvent was removed under reduced pressure and the crude product was purified by silica gel chromatography with eluting (PE: CH<sub>2</sub>Cl<sub>2</sub> = 3:1) to give **TP-BT-TP** as a solid (0.56 g, 47%). <sup>1</sup>H NMR (300 MHz, CD<sub>2</sub>Cl<sub>2</sub>) δ 8.49 (d, *J* = 3.9 Hz, 2H), 8.45 (s, 2H), 7.47 (d, *J* = 3.9 Hz, 2H), 4.87 (t, *J* = 6.9 Hz, 4H), 2.19 (m, 4H), 1.60–1.00 (m, 82H), 0.86 (m, 12H). <sup>13</sup>C NMR (75 MHz, CDCl<sub>3</sub>) δ 147.0, 145.0, 143.3, 141.1, 140.4, 138.3, 132.0, 126.1, 105.2, 57.6, 37.2, 33.0, 33.1, 32.0, 30.5, 30.1, 29.7, 29.6, 29.4, 26.7, 23.7, 22.7, 14.2. HR-MALDI-TOF: [M+H]<sup>+</sup> calcd for C<sub>68</sub>H<sub>109</sub>Br<sub>2</sub>N<sub>8</sub>S<sub>2</sub>: 1261.65630, found: 1261.65486.

**Polymer Synthesis:**



**PTBT-FBT: TP-BT-TP** (100.0 mg, 0.079 mmol), 5,5'-bis(trimethylstannyl)-3,3'-difluoro-2,2'-bithiophene (41.8 mg, 0.079 mmol), Pd<sub>2</sub>(dba)<sub>3</sub> (2.2 mg), P(*o*-tol)<sub>3</sub> (5.8 mg), and chlorobenzene (6 mL) were added to a Schlenk tube. The tube was charged with argon through a freeze-pump-thaw cycle for three times. The mixture was stirred for 12 h at 130 °C, cooled down to room temperature, and poured into methanol (100 mL) and stirred for 3 h. The precipitated product was filtered and purified via Soxhlet extraction with methanol (10 h), acetone (10 h), hexane (10 h), and was finally collected with chloroform. The chloroform fraction was concentrated by evaporation and precipitated into methanol (100 mL) and filtered off to afford the polymer (94 mg, 91%). GPC: *M*<sub>n</sub> = 21.0 kDa, *M*<sub>w</sub> = 50.0 kDa, PDI = 2.38. Anal. calcd. for C<sub>76</sub>H<sub>110</sub>F<sub>2</sub>N<sub>8</sub>S<sub>4</sub>: C 70.11, H 8.52, N 8.61; found: C 70.03, H 8.64, N 8.83.

## 2.Experimental details

Nuclear magnetic resonance (NMR) spectra were recorded on a Bruker DMX-300 (300 MHz) spectrometer. <sup>1</sup>HNMR chemical shifts were referenced to internal tetramethylsilane (TMS, 0 ppm). High-resolution matrix assisted laser desorption/ionization time-of-flight (HR-MALDI-TOF) mass spectra were collected on an Autoflex III (Bruker Daltonics Inc.) MALDI-TOF spectrometer. Molecular weights were determined by gel permeation chromatography (GPC) at 150 °C on a PL-220 system using 1,2,4-trichlorobenzene as the eluent. TGA measurements were carried out on a PerkinElmer series 7 thermal analysis system under N<sub>2</sub> at a heating rate of 10 °C min<sup>-1</sup>. UV-vis absorption spectra were measured on polymer solutions in ODCB and polymer films cast onto quartz glass using a Jasco-570 spectrophotometer. CV was carried out on an electrochemical workstation (CHI660c) using a three-electrode cell. The glassy carbon electrode coated with a thin film layer of polymer was used as the working electrode. Ag/AgCl (Ag in a 0.01 mol/L KCl) electrode was used as the reference electrode. Platinum wire was used as the counter electrode. Anhydrous and N<sub>2</sub> saturated solution 0.1 M tetrabutylammonium hexafluorophosphate (*n*-Bu<sub>4</sub>NPF<sub>6</sub>) in acetonitrile was employed as the electrolyte. The scan rate was 0.1 V/s. The morphologies of polymer films were characterized by a Dimension Veeco V AFM. The tapping mode was utilized. All samples were fabricated on Si/SiO<sub>2</sub>. 2D-GIWAXS was performed on 1W1A Station of Beijing Synchrotron Radiation Facility (λ = 1.54 Å).

The linear fitting equation for calculating the limit of detection (LOD):

For melamine analytes:

$$\lg Y = 0.11484 \lg x + 1.55266$$

For cimaterol analytes:

$$\lg Y = 0.12895 \lg x + 1.06851$$

For dinitolamide analytes:

$$\lg Y = 0.15075 \lg x + 0.88754$$

### 3.Theoretical calculation

The energy levels of PTBT-FBT and veterinary endectocides, including melamine, cimaterol and dinitolamide, are calculated by the density functional theory (DFT) as carried out in the Vienna ab initio simulation Package (VASP)<sup>[2-3]</sup>. The projected augmented wave (PAW) method<sup>[4]</sup> is used to study the interaction between the ionic cores and valence electrons. The Perdew-Burke-Ernzerhof (PBE) generalized gradient approximation (GGA) is made use of the exchange correlation functional<sup>[5]</sup>. To obtain the accurate energy levels of the polymers, the Heyd-Scuseria-Ernzerhof screened hybrid density functional (HSE06) is used<sup>[6]</sup>. Prior to the calculation of the energy levels, the structures of PTBT-FBT and veterinary endectocides are fully optimized until the force on each atom is less than 0.01 eV/Å. The distance between imaginary polymer chains is set to be larger than 10 Å to avoid their interaction. Because of the long unit cell along the polymer chain direction, only Gamma point in the Monkhorst-Pack scheme is used in the calculation<sup>[7]</sup>.

The binding energies of cimaterol and dinitolamide molecules to the TP and 2FBT positions of the PTBT-FBT polymer, referred to as model A for TP and model B for 2FBT, respectively, are calculated, respectively. For model A (in Figure S17), it showed that strong hydrogen bonds with bond lengths of 2.2 Å and 2.5 Å between a hydrogen atom of the analyte molecule and a nitrogen atom of the TP group in the PTBT-FBT polymer is formed, respectively. In addition, one extra relatively weak hydrogen bond between cimaterol molecule and the PTBT-FBT polymer is formed, and two extra relatively weak hydrogen bonds between dinitolamide molecule and the PTBT-FBT polymer are formed. In comparison, four relatively weak hydrogen bonds were formed in model B between two hydrogen atoms of the cimaterol and dinitolamide molecules and two fluorine and two sulfur atoms of the 2FBT group in the PTBT-FBT polymer, respectively (in Figure S17). Because of the strong hydrogen bond in model A, the corresponding binding energies for model A (0.423 eV and 0.358 eV) are higher than that for model B (0.293 eV and 0.328 eV). At room temperature, the adsorption possibility ratio between model A and model B can be estimated to be  $e^{\frac{\Delta E}{k_B T}} \approx 152$  and 3, where  $\Delta E$  is adsorption energy difference,  $k_B$  is Boltzmann constant and T is temperature. This result demonstrated that the analytes were primarily absorbed on the polymer film surface at TP through hydrogen-bonding formation.

The Heyd-Scuseria-Ernzerhof screened hybrid density functional (HSE06) was used to calculate the HOMO and LUMO orbitals of PTBT-FBT with and without the adsorption of melamine.<sup>[6]</sup>

### 4.Device fabrication and testing

The substrates for OFET fabrication were purchased from Peking University in which heavily doped silicon was used as gate electrodes, 300-nm-thick thermally grown SiO<sub>2</sub> as dielectric layer and 30-nm-thick Au as source and drain electrodes. Before the off-center spin-coating process, the Si/SiO<sub>2</sub> substrates were firstly immersed in acetone for 2 hours and then ultrasonicated for 5 min, followed by drying in a nitrogen flow. Then, the clean Si/SiO<sub>2</sub> substrates were dipped in a mixture of concentrated sulfuric acid and hydrogen peroxide (a volume ratio of 7:3) for 5 min. After that, these substrates were cleaned by 5-min ultrasonication in secondary water, acetone and isopropyl alcohol, respectively, followed by again dried in a nitrogen flow. After UVO treatment on the surface of the Si/SiO<sub>2</sub> substrate for 20 min, the substrates were modified self-assembled monolayer (SAMs) octadecyltrichlorosilane (OTS) by vapor deposition method in oven at 120 C for 3 hours. After that, the OTS-modified substrates were cleaned by 5-min ultrasonication in normal hexane, trichloromethane and isopropyl alcohol respectively. Ultimately, the polymer PTBT-FBT with different solution concentrations (0.7-5 mg mL<sup>-1</sup>) in o-dichlorobenzene was deposited on the surface-modified Si/SiO<sub>2</sub> substrates based on the off-center method at a spin-coating speed of 5000 rpm, aiming to obtain different-thickness polymer films. Subsequently, the resulting polymer films were subjected to annealing treatment at 150 C for 10 min to remove the residual o-dichlorobenzene solvent. A Keithley 4200-SCS was used for all electrical measurements to PFET-based LDPNs solid sensors in a glovebox.

## 5. Figures S1-S19 and Table S1-S6

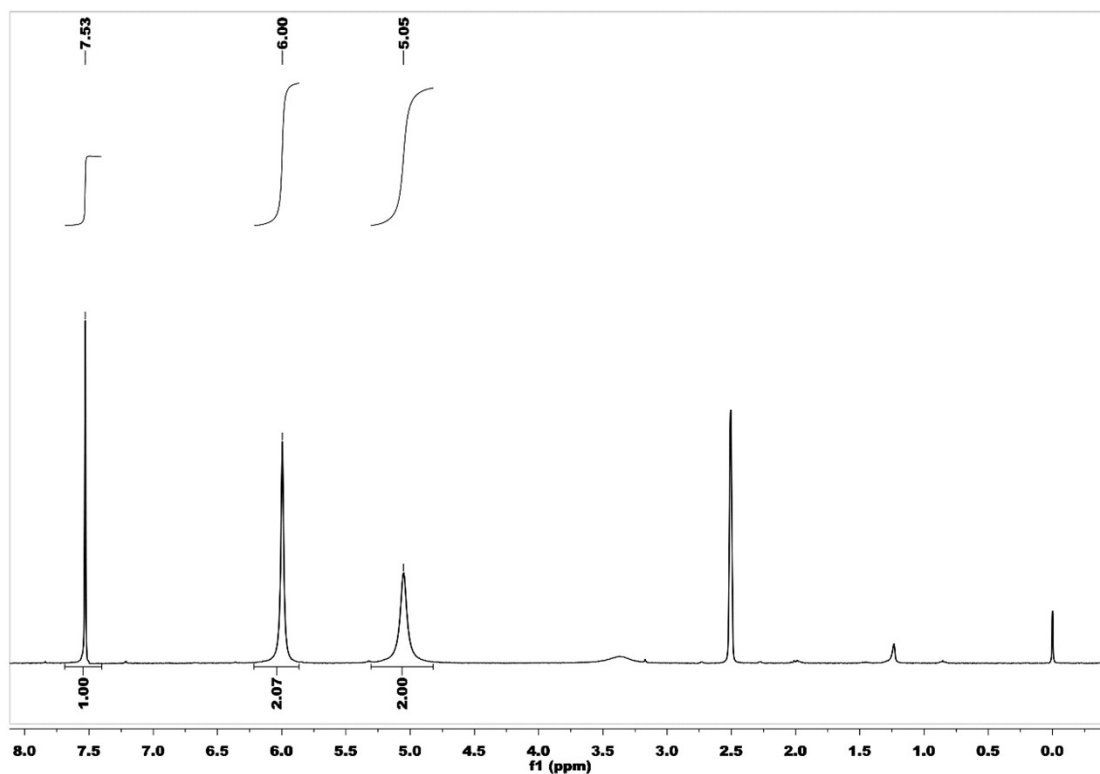


Figure S1. The <sup>1</sup>H NMR spectrum of Compound 2.

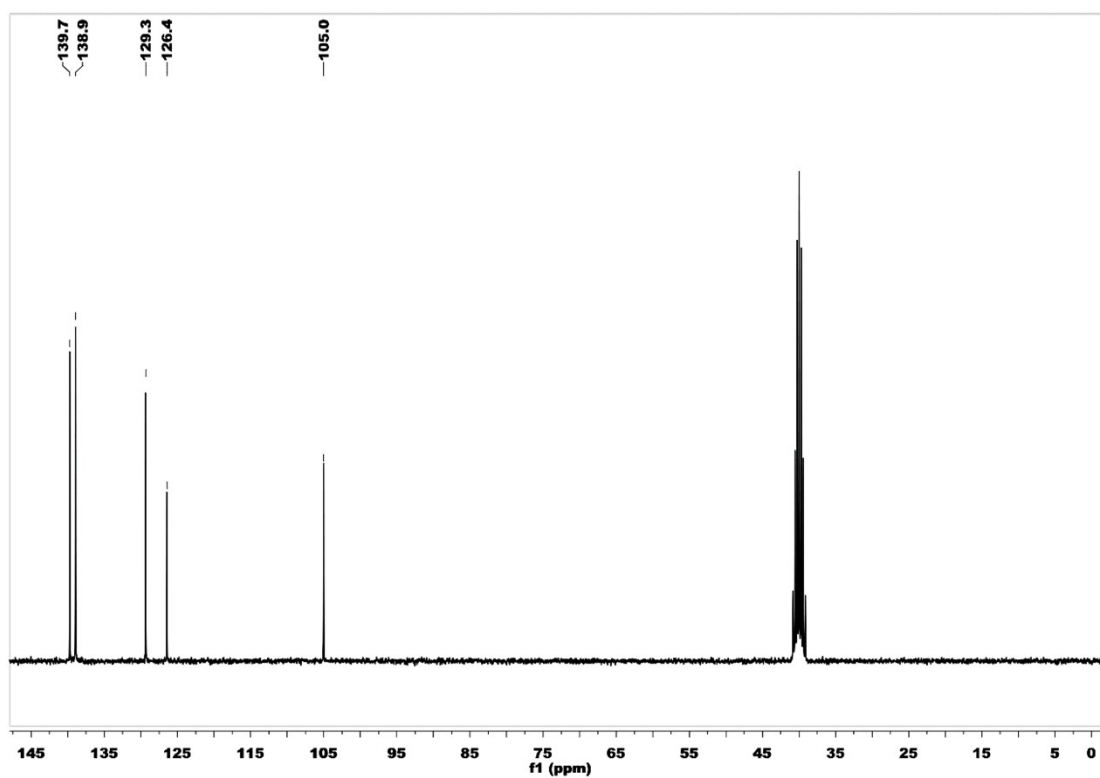


Figure S2. The  $^{13}\text{C}$  NMR spectrum of Compound 2.

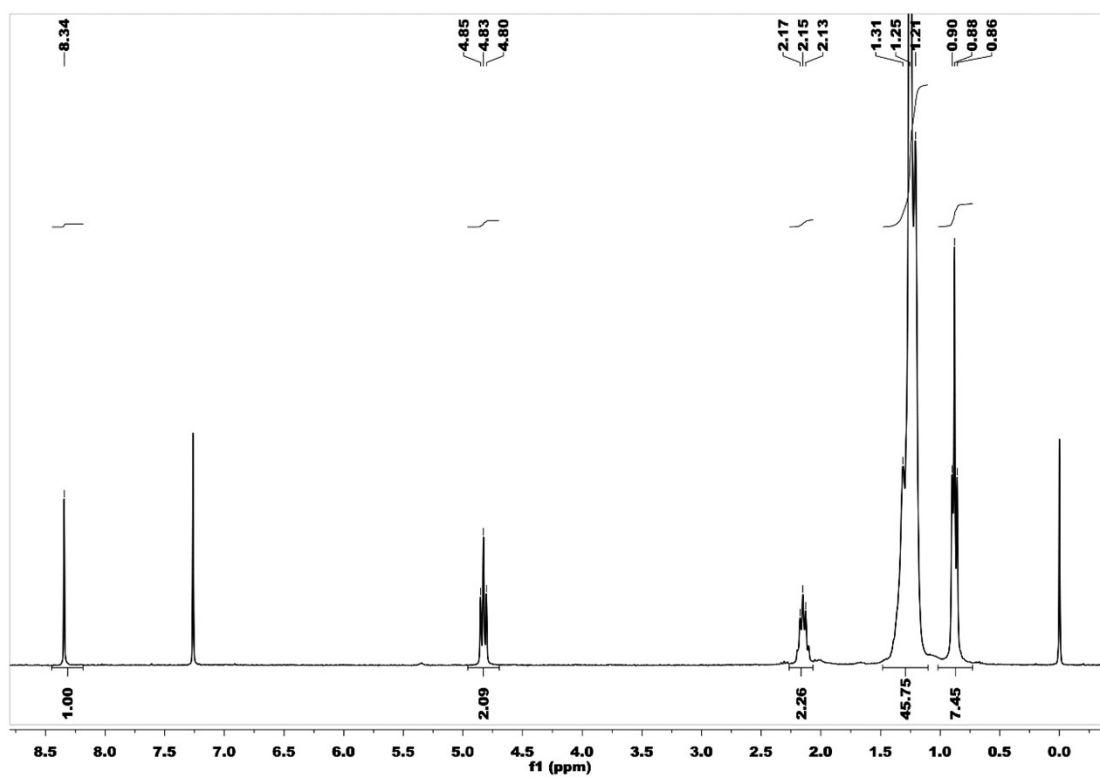


Figure S3. The  $^1\text{H}$  NMR spectrum of Compound 4.

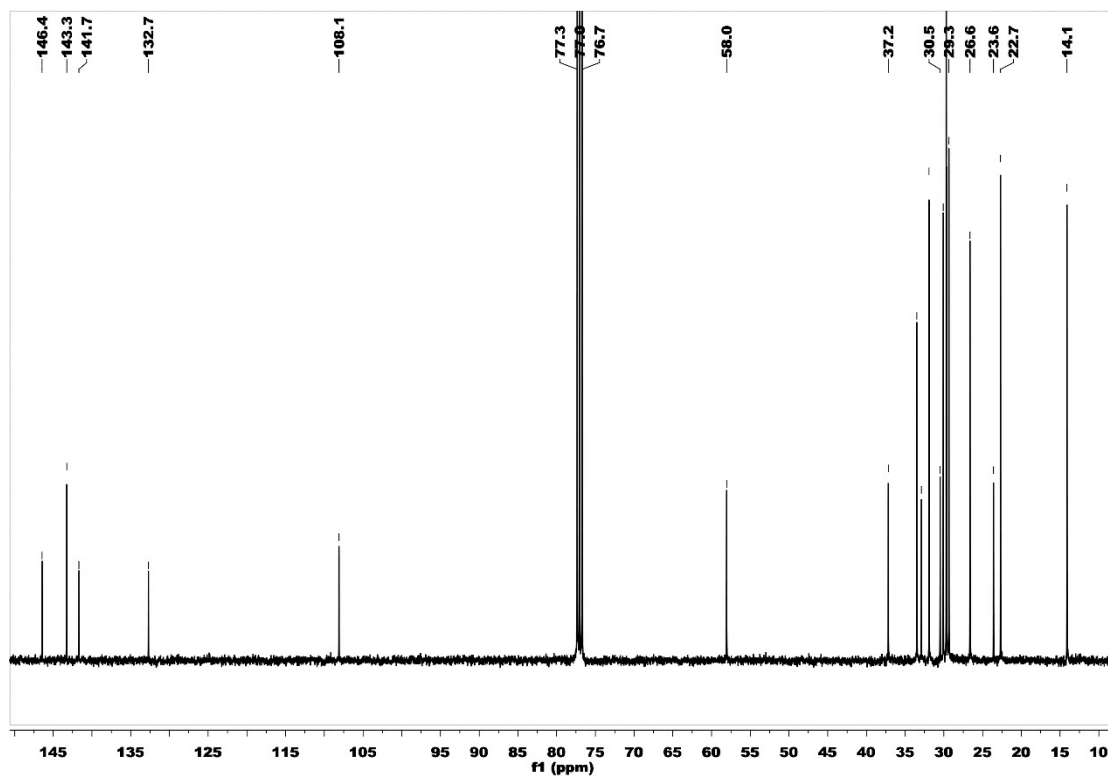


Figure S4. The  $^{13}\text{C}$  NMR spectrum of Compound 4.

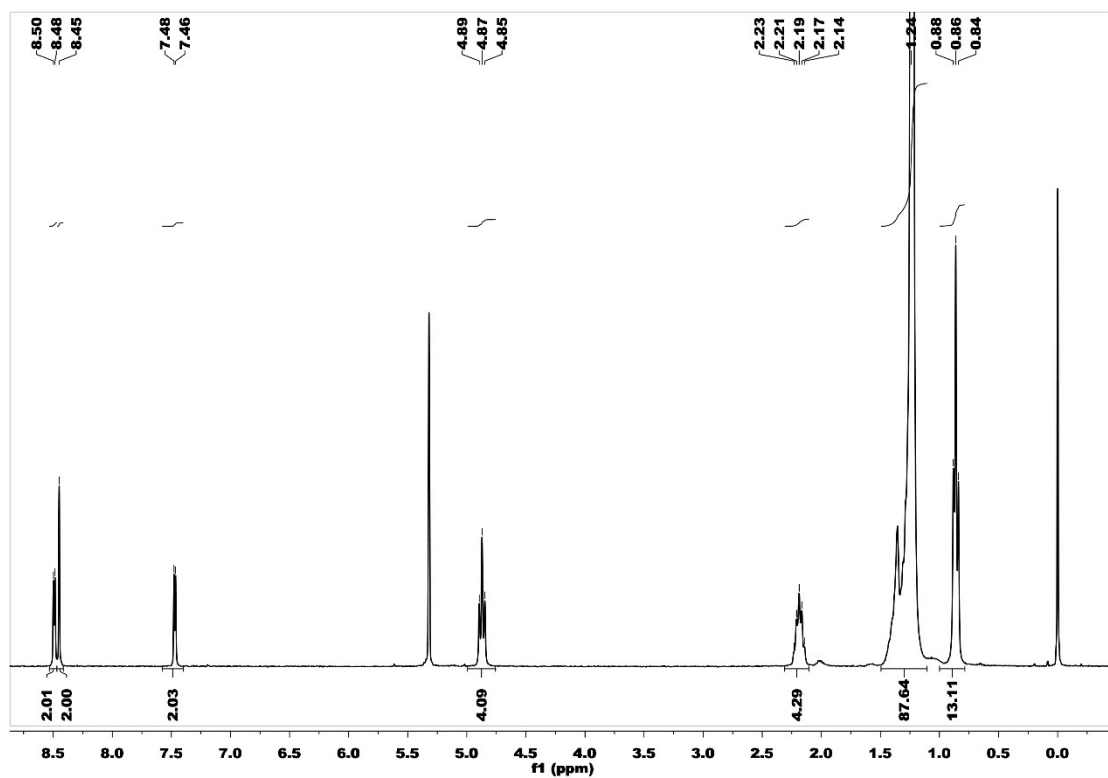


Figure S5. The  $^1\text{H}$  NMR spectrum of TP-BT-TP



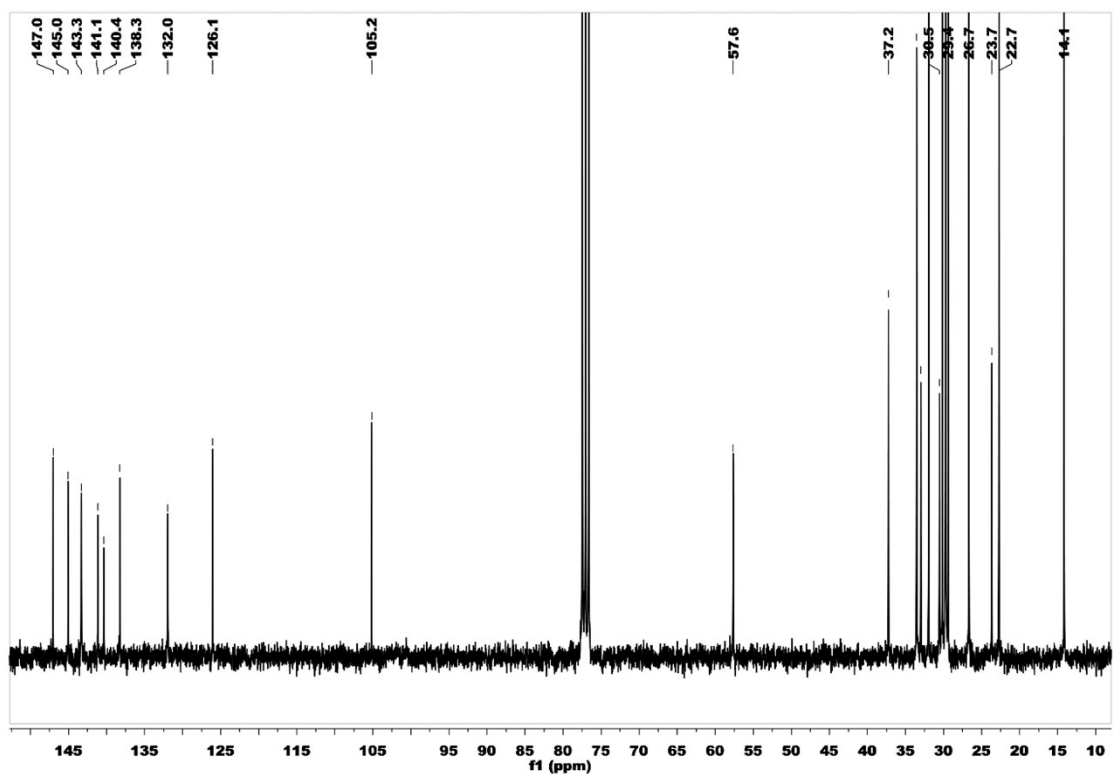


Figure S6. The  $^{13}\text{C}$  NMR spectrum of TP-BT-TP.

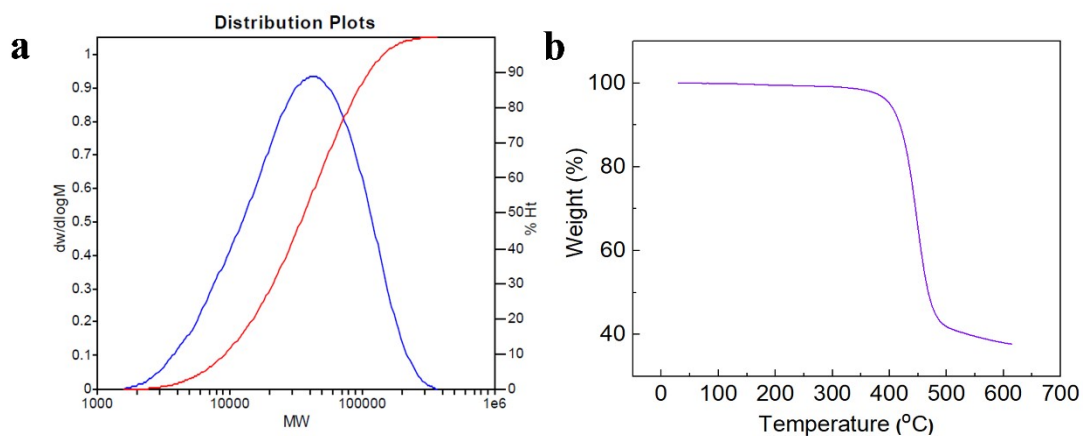


Figure S7. (a) Gel permeation chromatography (GPC) trace of PTBT-FBT. (b) Thermal gravity analyse of PTBT-FBT.

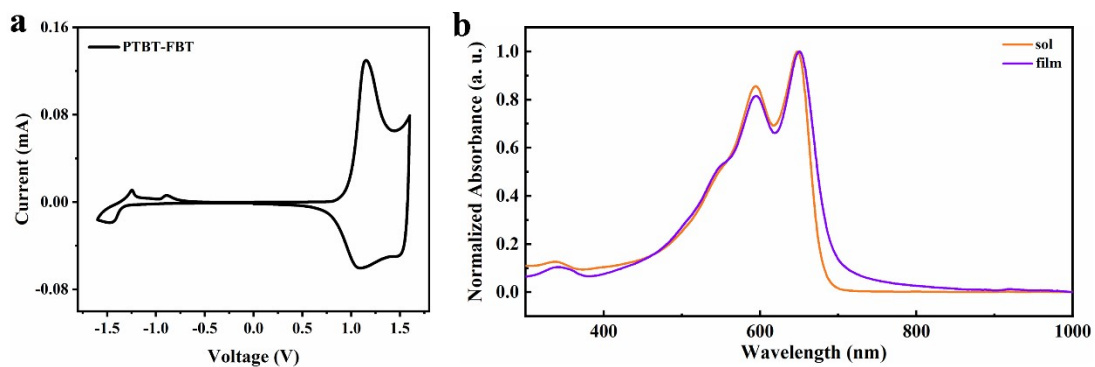
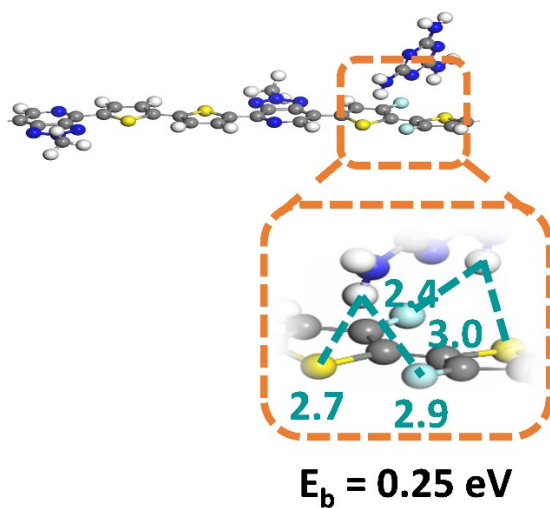
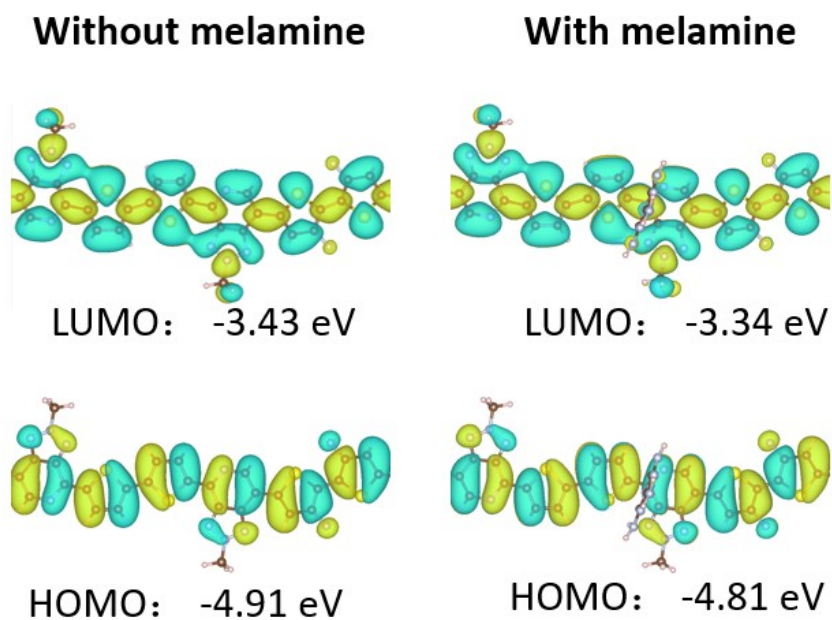


Figure S8. (a) The CV result of PTBT-FBT. (b) UV-Vis spectra of PTBT-FBT.



**Figure S9.** Structures and corresponding binding energies of a melamine molecule adsorbed to BT positions of the PTBT-FBT polymer.



**Figure S10.** DFT calculated LUMO and HOMO of PTBT-FBT without (left panels) and with (right panels) the presence of melamine.

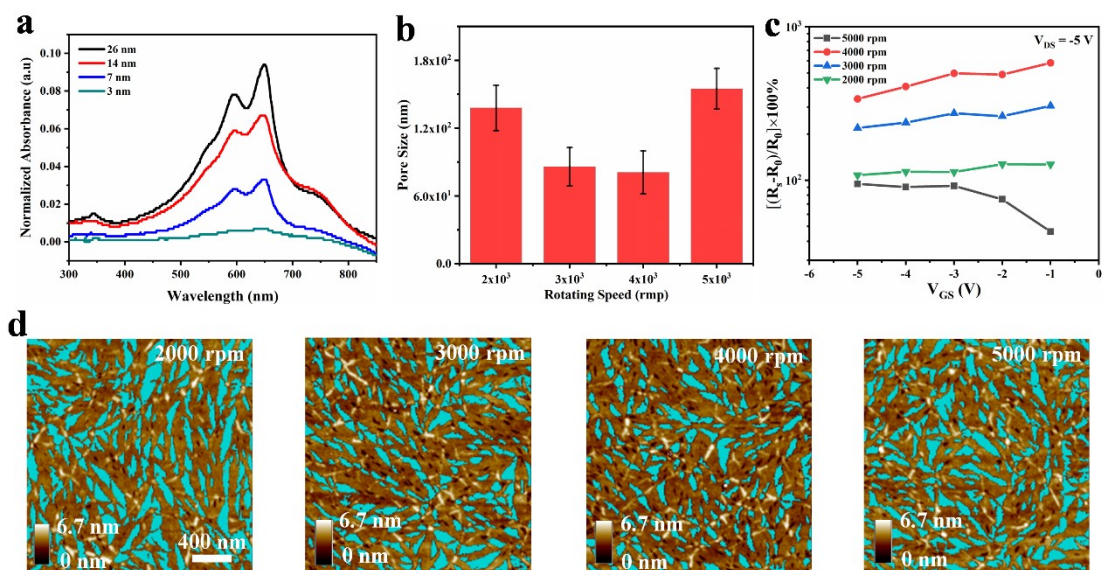


**Figure S11.** (a) UV-Vis absorption spectra of PTBT-FBT deposited on quartz wafers by off-centering at different concentrations (0.7, 1, 3, and 5 mg mL<sup>-1</sup>). (b) The relationship between the resistance response and rotating speed. (c) The sensitivity of resistance response against the rotating speed under solution concentration of 0.7 mg mL<sup>-1</sup> at gate voltage of -5 V and source-drain voltage of -5 V. (d) The particle analysis of low-dimensional network polymer films prepared by adjusting rotating speed ranging from 2000 rpm to 5000 rpm using the AFM processing software.

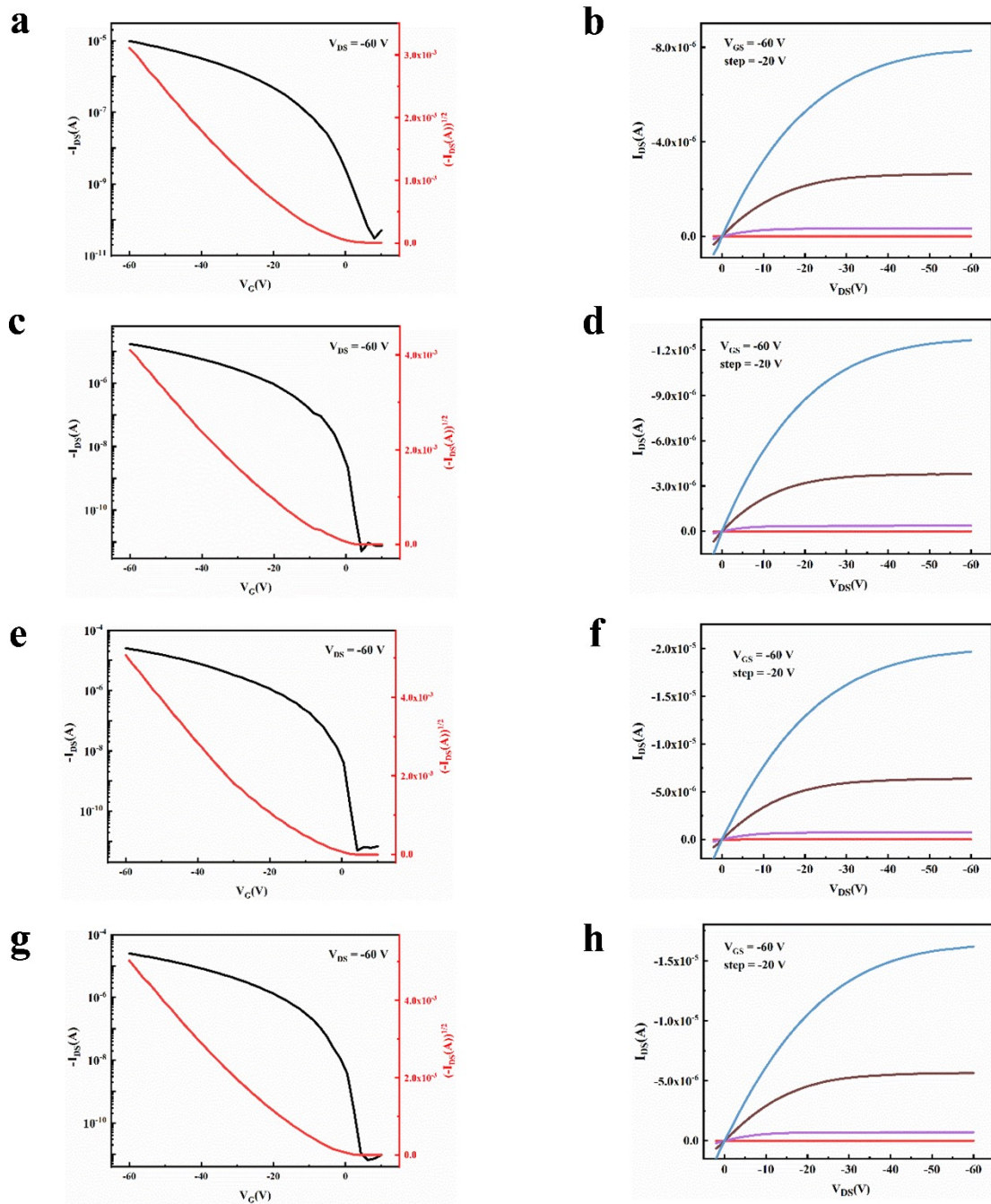


**Figure S12.** The transfer and output characteristics of BCBG transistors at different film thicknesses prepared by off-center process. a) – b) 3nm. c) – d) 6nm. e) – f) 12nm. g) – h) 24nm.

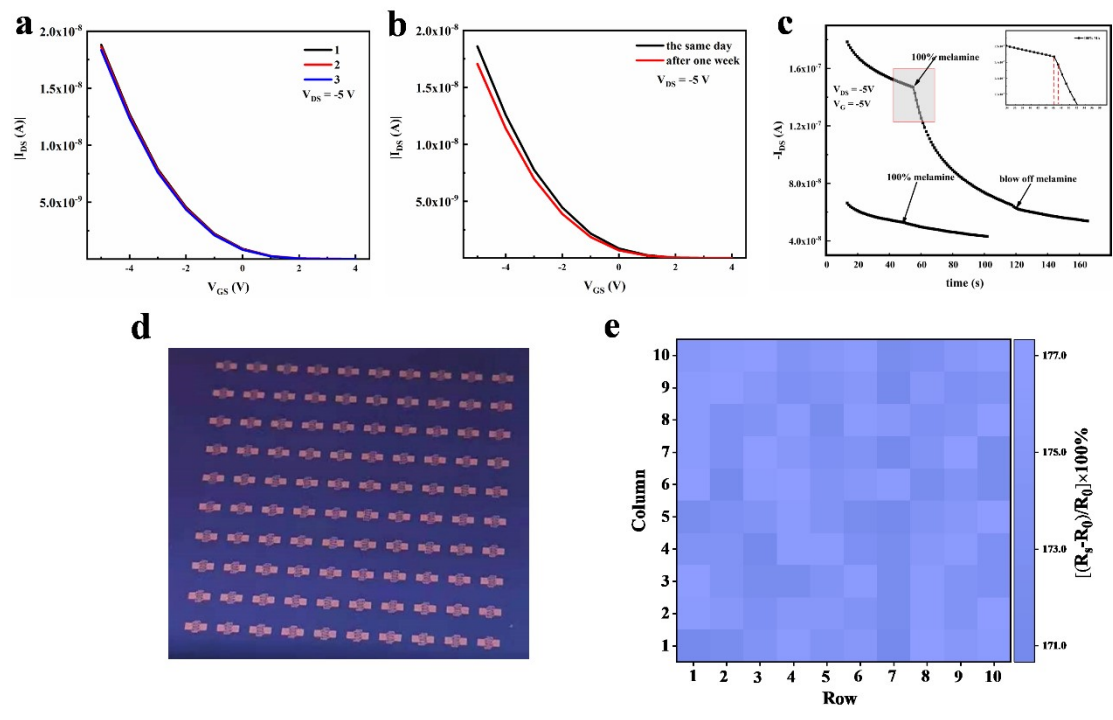


**Figure S13.** The repeatability and stability tests of solid sensing devices under  $V_{gs} = -5$  V and  $V_{ds} = -5$  V. (a) The cycle test transfer curve of single device before sensing process. (b) The shelf life of the sensor. (c) The current changes as functions of applied melamine powders and blow off melamine. (d) The device array of 10 column  $\times$  10 row, with channel length of 1400  $\mu$ m and channel width of 50  $\mu$ m. (f) The resistance response uniformity of 10 column  $\times$  10 row sensing array corresponding to the devices in (d) exposed under pure melamine powders.

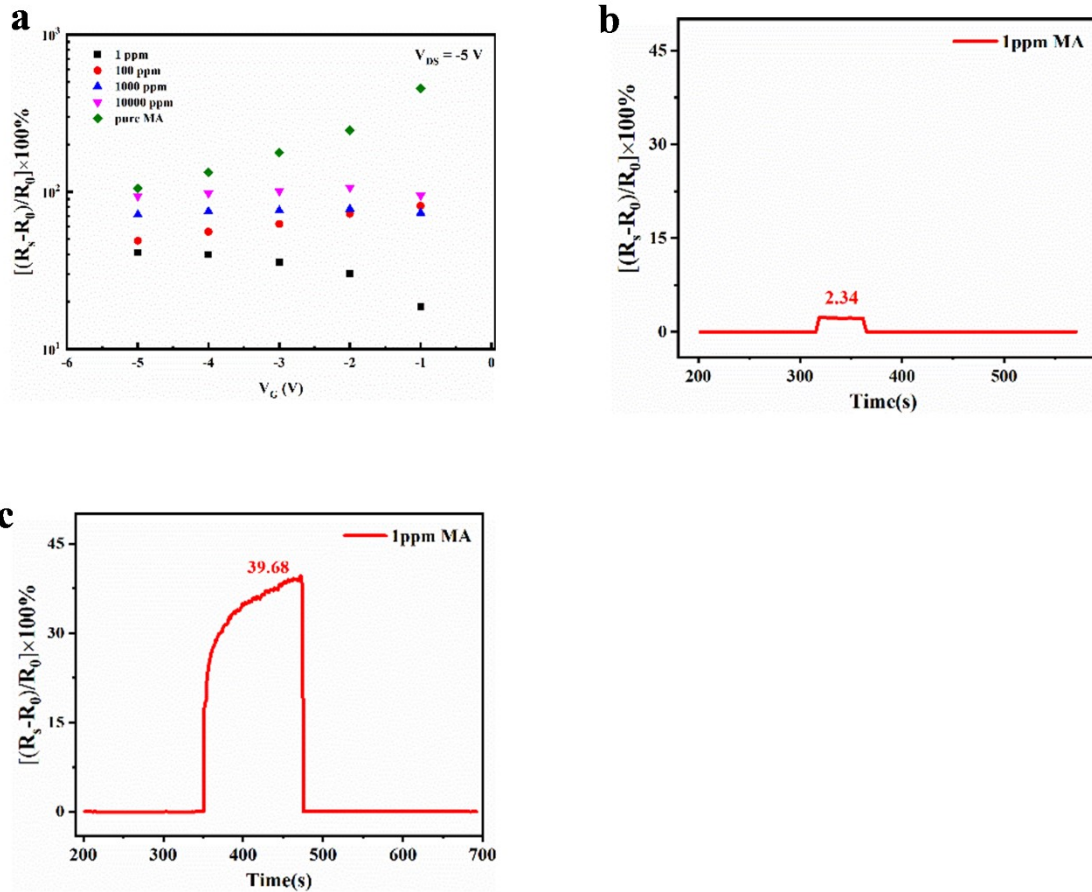


**Figure S14.** (a) The resistance response of melamine upon exposure to various powders concentration under  $V_{gs}$  of  $-5 \text{ V}$  and  $V_{ds}$  of  $-5 \text{ V}$ . (b-c) The resistance response of two-terminal and three-terminal sensors upon exposure to melamine powders at a concentration of  $1 \text{ ppm}$  under  $V_{gs}$  of  $-5 \text{ V}$  and  $V_{ds}$  of  $-5 \text{ V}$ .

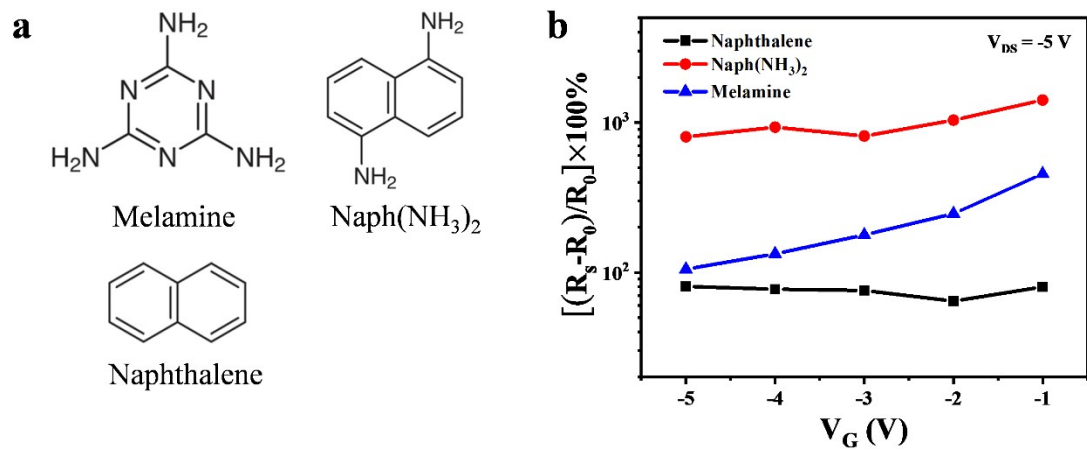


**Figure S15.** (a) The chemical structures of melamine, Naph(NH<sub>3</sub>)<sub>2</sub> and Naphthalene. (b) The sensitivity comparison diagram of melamine, Naph(NH<sub>3</sub>)<sub>2</sub> and Naphthalene under  $V_{gs}$  of  $-5 \text{ V}$  and  $V_{ds}$  of  $-5 \text{ V}$ .

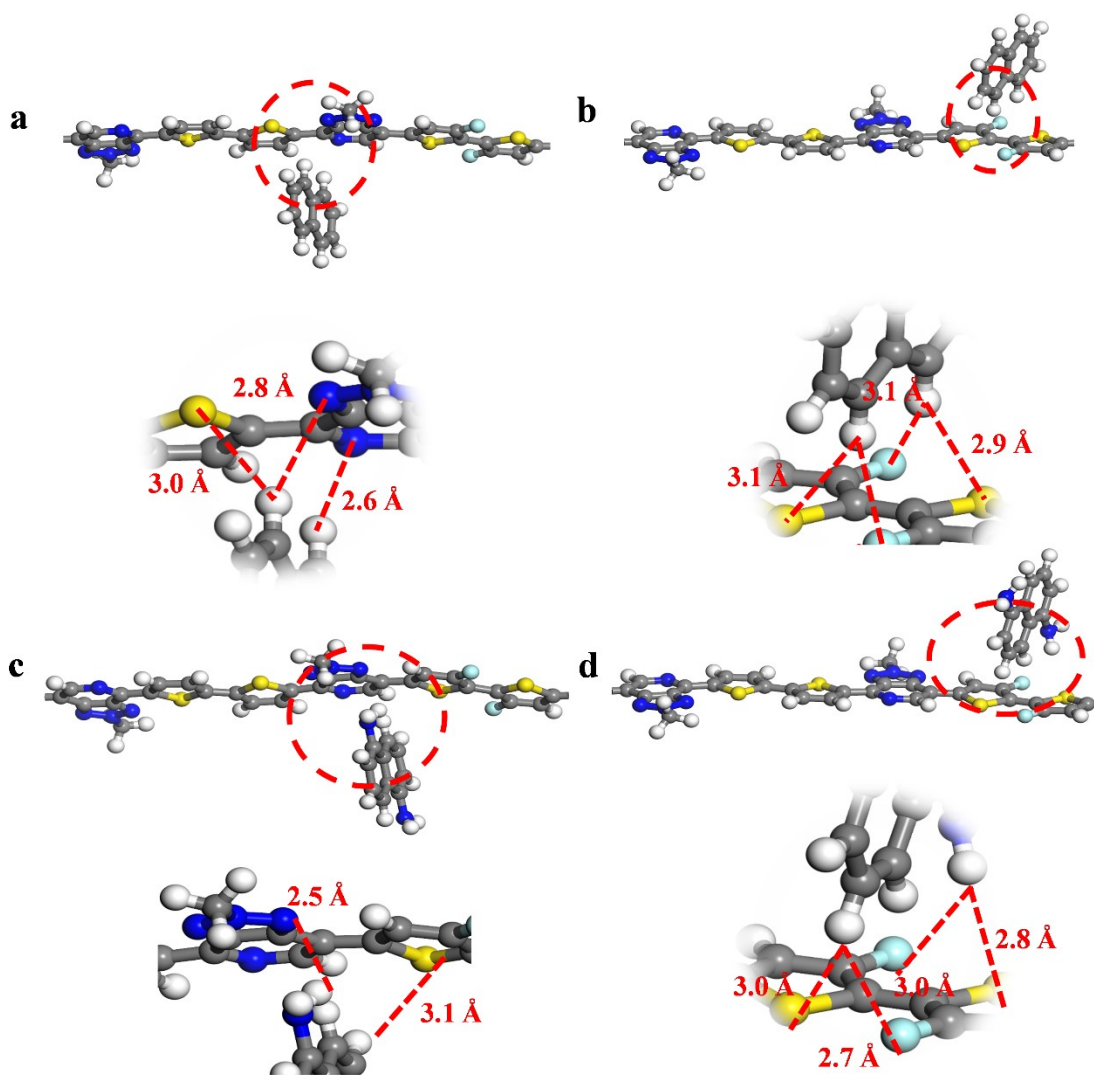


**Figure S16.** Structures and corresponding binding energies of (a) a Naphthalene molecule and (c) a Naph(NH<sub>3</sub>)<sub>2</sub> adsorbed to TP position of the PTBT-FBT polymer. Structures and corresponding binding energies of (b) a Naphthalene molecule and (d) a Naph(NH<sub>3</sub>)<sub>2</sub> molecule adsorbed to 2FBT position of the PTBT-FBT polymer.

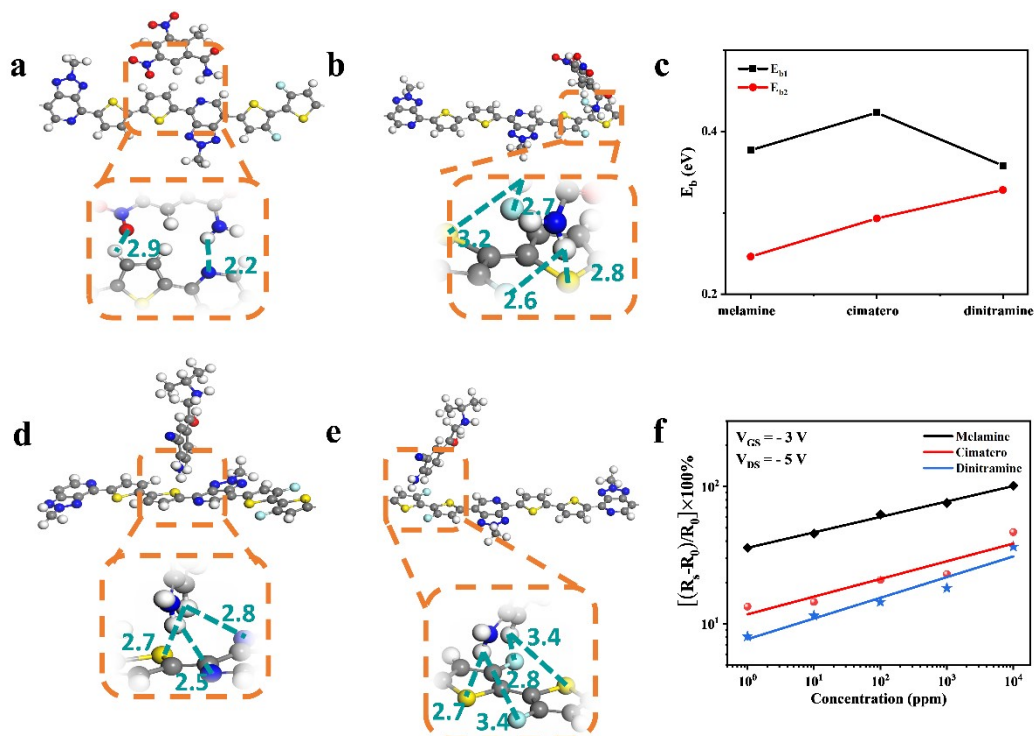


**Figure S17.** Structures and corresponding binding energies of a cimetrol molecule adsorbed to (a) TP positions and (b) 2FBT positions of the PTBT-FBT polymer. (c) Binding energies between polymer and veterinary endectocides:  $E_{b1}$  corresponding to the binding energies at TP-BT;  $E_{b2}$  corresponding to the binding energies at 2FBT. Structures and corresponding binding energies of a dinitolamide molecule adsorbed to (d) TP positions and (e) 2FBT positions of the PTBT-FBT polymer. (f) The sensitivity of resistance response against the concentration of melamine, cimetrol and dinitolamide powders.

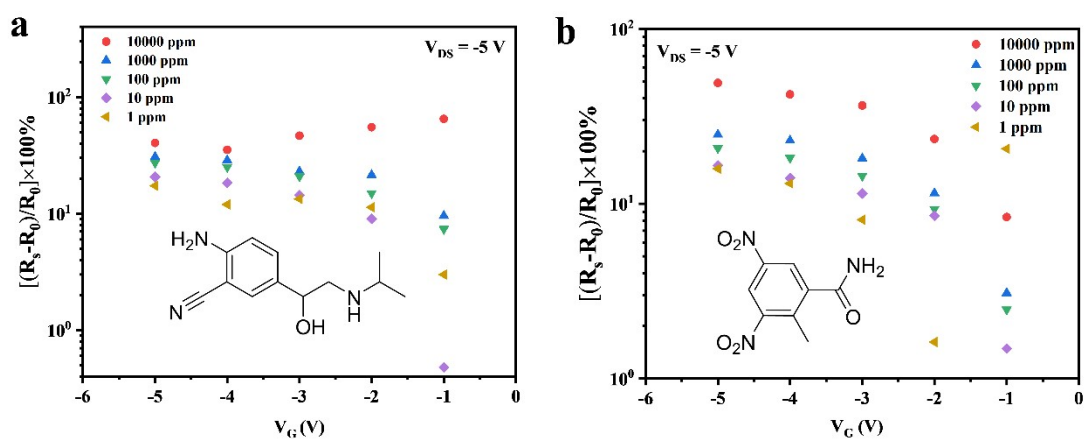


**Figure S18.** The resistance response of PFET-based LDNPs solid sensors upon exposure to (a) cimetrol and (b) dinitolamide powders at various concentration under gate voltage of  $-5\text{ V}$  and source – drain voltage of  $-5\text{ V}$ .



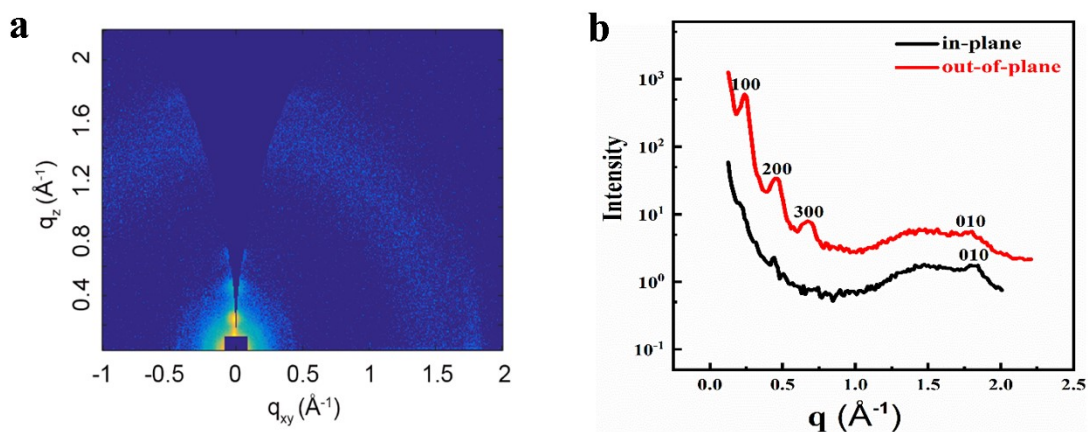


**Figure S19.** (a) Two-dimensional GIWAXS figure of PTBT-FBT prepared by off-center process. (b) GIWAXS line profiles of PTBT-FBT.

**Table S1.** Adsorption energies between polymer and molecules at TP-BT.

Name	$E_{\text{total}}$ (eV)	$E_{\text{poly}}$ (eV)	$E_{\text{mole}}$ (eV)	$E_{\text{binding}}$ (eV)
Melamine	-492.315	-391.555	-100.383	0.377
Cimatero	-543.726	-391.555	-151.748	0.423
Dinitramine	-590.645	-391.555	-198.207	0.358
Naph	-511.637	-391.555	-119.884	0.198 eV
Naph(NH <sub>3</sub> ) <sub>2</sub>	-536.102	-391.555	-144.298	0.249

**Table S2.** Adsorption energies between polymer and molecules at 2FBT.

Name	$E_{\text{total}}$ (eV)	$E_{\text{poly}}$ (eV)	$E_{\text{mole}}$ (eV)	$E_{\text{binding}}$ (eV)
Melamine	-492.184	-391.555	-100.383	0.246
Cimatero	-543.596	-391.555	-151.748	0.293
Dinitramine	-590.218	-391.555	-198.207	0.328
Naph	-511.621	-391.555	-119.884	0.182
Naph(NH <sub>3</sub> ) <sub>2</sub>	-536.102	-391.555	-144.298	0.249

**Table S3.** The equivalent mean diameter as function of rotating speed.

Rotating speed (rpm)	2000	3000	4000	5000
Equivalent mean diameter(nm)	49.038	37.329	35.973	41.273
Coverage (%)	66	77	82	71

**Table S4.** The hole mobility of OFET based on different film thickness.

Thickness (nm)	3	6	12	24
Mobility(cm <sup>2</sup> /Vs)	0.027	0.048	0.062	0.056

**Table S5.** The polymer energy level.

E <sub>g</sub> (eV)	HOMO(eV)	LUMO(eV)
1.77	-5.23	-3.46

<sup>a</sup>Determined from the onset of thin-film absorption; <sup>b</sup>Determined from the onset of oxidation potential of cyclic voltammetry; <sup>c</sup>Calculated using the equation  $E_g = \text{LUMO} - \text{HOMO}$ .

**Table S6.** The molecular weight of PTBT-FBT from GPC.

M <sub>n</sub>	M <sub>w</sub>	PDI
21.0 kDa	50.0kDa	2.38

## 6. Reference

- [1] S. Chaurasia, W.-I. Hung, H.-H. Chou, J. T. Lin, *Organic Letters* 2014, **16**, 3052-3055.
- [2] Kresse, G.; Hafner, J., *Phys. Rev. B* 1993, **48**, 13115-13118.
- [3] Kresse, G.; Furthmuller, J., *Comput. Mater. Sci.* 1996, **6**, 15-50.
- [4] Kresse, G.; Joubert, D., *Phys. Rev. B* 1999, **59**, 1758-1775.
- [5] Perdew, J. P.; Burke, K., *Phys. Rev. Lett.* 1996, **77**, 3865-3868.
- [6] Krukau, A. V.; Vydrov, O. A.; Izmaylov, A. F.; Scuseria G. E. *J. Chem. Phys.* 2006, **125**, 224106.
- [7] Monkhorst, H. J.; Pack, J. D., *Phys.Rev. B* 1976, **13**, 5188.